

# SPACE-BORNE PROFILING OF ATMOSPHERIC THERMODYNAMIC VARIABLES WITH RAMAN LIDAR

Paolo Di Girolamo<sup>1\*</sup>, Andreas Behrendt<sup>2</sup>, Volker Wulfmeyer<sup>2</sup>

<sup>1</sup>*Scuola di Ingegneria, Università degli Studi della Basilicata, Italy, \*Email: digirolamo@unibas.it*

<sup>2</sup>*Institut für Physik und Meteorologie, Universität Hohenheim, Germany*

## ABSTRACT

The performance of a space-borne water vapour and temperature Raman lidar has been simulated, with a specific attention to the Earth Explorer Missions in the frame of ESA's Living Planet Program. We report simulations under a variety of atmospheric scenarios, demonstrating the capability of a space Raman lidar to provide global-scale water vapour and temperature measurements in the troposphere with an accuracy fulfilling most observational requirements for numerical weather prediction (NWP) and climate research.

## 1 INTRODUCTION

An appropriate understanding and prediction of the Earth's temperature and water distributions is fundamental for a sustainable development of the Earth system. Unfortunately, our understanding of the water and energy cycles still shows critical gaps on all temporal and spatial scales. This is mainly due to a lack of measurement of water vapour and temperature profiles - hereafter called thermodynamic profiles - with high accuracy and high temporal-spatial resolution, especially in the lower troposphere.

Wulfmeyer *et al.* (2015) [1] demonstrated that the availability of global scale measurements of 3-dimensional thermodynamic profiles would have a revolutionary impact on our Earth system understanding in four key research areas: i) radiative transfer, with resulting implications on regional and global water and energy budgets, ii) land-atmosphere feedback including the surface energy balance closure in dependence of soil properties and land cover, iii) mesoscale circulations and convection initiation, and (iv) convective-scale data assimilation.

These observational gaps can only be closed by the development and operation of a new active remote sensing system in space based on the

Raman lidar technique (Wulfmeyer *et al.*, 2015). In fact, combining vibrational and rotational Raman signals, simultaneous accurate and high-resolution measurements of water vapour and temperature profiles are possible. An instrumental concept is proposed here for a space-borne system based on the experience and know-how gained with the development and operation of several existing ground-based instruments ([2], [3]; [4], [5], [6], [7]; [8]) and airborne instruments [9]. Possible instrumental specifications for the different sub-systems are proposed to simulate the performances of a space-borne water vapour and temperature Raman lidar under a variety of environmental and atmospheric scenarios. For this purpose, different atmospheric reference models covering different climatic regions and seasons, as well as a variety of solar illumination conditions, were considered.

Observational requirements for NWP and climate research to be fulfilled by networks of satellite remote sensors, with a specific focus on the lower troposphere, have been identified by Wulfmeyer *et al.* (2015) [1]. The vertical resolution should be sufficiently high to resolve temperature and moisture gradients in the lower troposphere. Measurements are required at meso-beta to meso-gamma scale resolution. The water vapour/temperature bias should be 2–5% (0.2–0.5 K) and the noise errors smaller than 10% (1 K) in each single vertical range bin. In order to have a significant impact on all four above-mentioned primary application fields, space-borne lidar measurements with a vertical and horizontal resolution of 200 m and 50 km are required.

## 2. METHODOLOGY AND SYSTEM CONCEPT

An analytical lidar simulator, developed at Università degli Studi della Basilicata [5], has been applied in this paper to assess the expected performances of a space-borne water vapour and

temperature Raman lidar system exploiting the vibrational and pure rotational Raman techniques in the ultraviolet (UV). The simulator allows to assess measurement quality in terms of both systematic and random measurement errors. The specifications of different lidar sub-systems have been assessed based on the application of the model.

Simulations consider a sun-synchronous low-Earth dusk/dawn orbit (inclination  $\sim 97$  degrees), with an orbiting height and speed of 450 km and 7 km/s, respectively [10]. A dawn-dusk orbit characterized by an ascending node crossing time of 6 h was selected. A  $3^\circ$  off-nadir transmission of the laser beam is considered to avoid specular reflections from ice crystals.

The statistical uncertainty affecting water vapour mixing ratio and temperature measurements are determined through error propagation from the estimates of the noise errors affecting the Raman lidar signals, the latter being determined from the application of Poisson statistics to the signals. In this regard, it is to be specified that the application of Poisson statistics to the lidar signals is well suited in case of data acquired in photon-counting or in analogue mode, in the latter case after conversion of the analogue signals into “virtual” counts [3].

Atmospheric parameters considered in the simulation include vertical profiles of pressure, temperature, and humidity from three selected atmospheric reference models (tropical atmosphere, sub-Arctic winter, and U.S. Standard Atmosphere), considered for both summer and winter, and the median aerosol extinction data from the ESA Aerosol Reference Model of the Atmosphere (ESA-ARMA, 1999 [11]).

An analytical expression for the daylight sky background signals collected in the various channels has been formulated and tested in Di Girolamo *et al.* (2006 [5]). This expression includes three distinct contributions: namely, a cloud-free atmospheric contribution, a surface contribution, and a cloud contribution. The cloud-free atmospheric contribution accounts for the scattering of solar radiation by atmospheric constituents (molecular species and aerosols), the surface contribution is associated with Earth surface reflection of direct solar radiation, and the

cloud contribution accounts for the cloud reflection of direct solar radiation. All three contributions depend on the solar zenith angle, with values largely increasing at small zenith angles. For this reason a sun-synchronous low Earth dusk-dawn orbit was selected for the simulations. Background contributions are proportional to the field of view of the receiving telescope (FOV) and this pushes in the direction to consider a very small FOV, compatibly with a reduced optical layout complexity and a large signal stability.

The Raman lidar is designed to collect four primary lidar signals: the water vapour vibrational Raman signal  $P_{H_2O}(z)$ , the high- and low-quantum-number rotational Raman signals,  $P_{lo}(z)$  and  $P_{Hi}(z)$ , and the elastic backscatter signal in the UV,  $P_{354.7}(z)$ . There is no need for the collection of the molecular nitrogen vibrational Raman signal  $P_{N_2}(z)$  as in fact an alternative temperature-insensitive reference signal ( $P_{ref}(z)$ ) can be obtained from the combination of the rotational Raman signals  $P_{lo}(z)$  and  $P_{Hi}(z)$  [2]. This set of detected signals allows for independent measurements of atmospheric temperature, the water vapour mixing ratio (and consequently relative humidity) and the particle backscattering and extinction coefficients at 354.7 nm, the latter two such as delivered by EarthCARE mission. Besides the above mentioned parameters, very valuable additional products can be independently measured: the true atmospheric boundary layer depth over land and the oceans derived by the high-vertical resolution temperature profiles and the geometric and optical properties of clouds.

The lidar transmitter will consist of a frequency-tripled, diode-laser pumped Nd:YAG laser with efficiency of  $>10\%$  and an average power in the UV (at 354.7 nm) of at least 250 W. The UV laser power required for the measurements can be achieved based on a new generation of pump chambers, with efficient pumping by diode lasers. The baseline to achieve the large UV laser powers required for these applications is represented by inclusion of several amplification stages. The implementation of diode laser pumping determines radiative or conductive cooling to be sufficient. Based on the electric power provided by the on-board solar arrays (2.5 kW) and an

overall electric-to-355-nm efficiency in excess of 10 %, a laser power of >250 W at 355 nm can be generated.

The receiver must consist of a large-aperture telescope and an extremely stable and highly efficient receiving unit for the collection of the rotational and vibrational Raman signals. Simulations indicate the need for a telescope with a diameter of 8 m. The development of large-aperture telescopes may consider different technological solutions, as the use of segmented deployable or inflatable optics. New technological concepts for large aperture, lightweight telescopes, using thin deployable active mirrors have been demonstrated for lidar applications [12]. Several glass materials (e.g. Zerodur) have been tested and demonstrated to have the appropriate low weight and thermal stability characteristics for this type of space application. Simulations indicate the need for a receiving field-of-view (full width half maximum) of just 80  $\mu$ rad. This requirement is a much more relaxed than the one considered for ADM (25  $\mu$ rad), strongly reducing complexity and improving signal stability. The selection of the Raman scattered signals will be based on the use of interference filters; different options for the filters' specifications are considered in the simulations [4,13]. Simulation results illustrated in this paper are based on filters' specifications in [4]. The present simulations consider photon detection based on the use of photomultipliers and refer to the specifications of commercially available UV photomultipliers, with UV quantum efficiencies of approx. 30%. However, accumulation charge-coupled devices (ACCDs), as for example those developed for ADM, may also be used, thus allowing to achieve even higher quantum efficiencies (up to 85%) and to further improving measurement accuracy.

### 3 SIMULATION RESULTS

Simulations reported in the present paper refer to a vertical and horizontal resolution of 200 m and 50 km, respectively. Based on this horizontal resolution, more than 500 thermodynamic profiles/hour can be collected, i.e., ~12,000 profiles/day (as opposed to ~1200 radiosonde launches available from the international upper-air network). Figure 1 illustrates the vertical profile

of the statistical uncertainty (precision) affecting water vapour mixing ratio measurements.

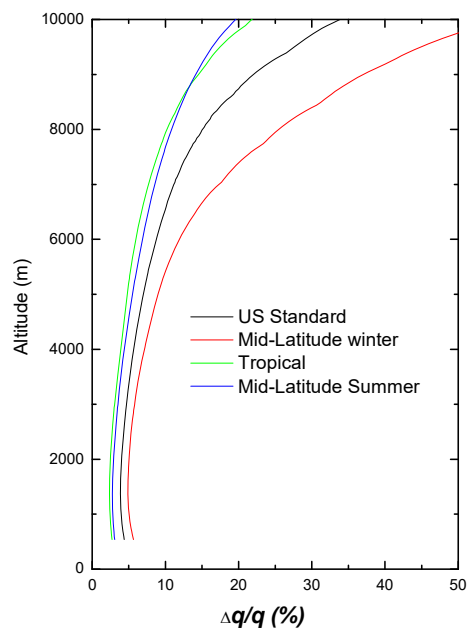


Figure 1: Vertical profile of the statistical uncertainty affecting water vapour mixing ratio measurements. The simulations consider four selected atmospheric reference models (tropical atmosphere, mid-latitude summer and winter, as well as U.S. Standard Atmosphere).

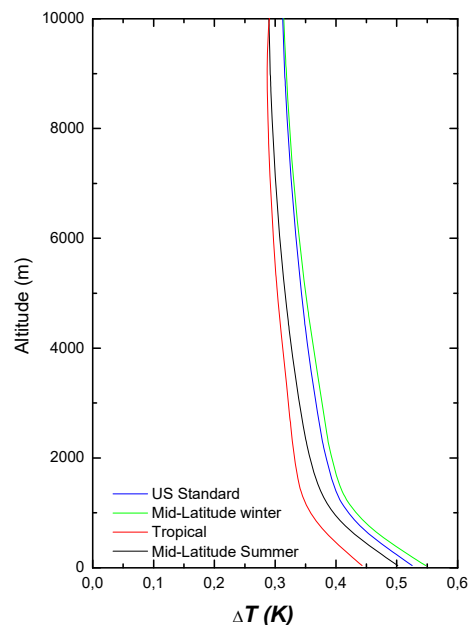


Figure 2: Vertical profile of the statistical uncertainty affecting temperature measurements. The present simulations consider the filters' specifications given in [4].

The simulations consider four different atmospheric reference models (tropical, mid-latitude summer and winter, as well as the U.S. Standard Atmosphere). Results in figure 1 reveal that the statistical uncertainty affecting water vapour mixing ratio has very small values throughout the boundary layer, with values not exceeding 5 % up to 3 km for three selected atmospheric reference models and < 10 % for all four. The statistical uncertainty is found to increase with altitude above 3 km, with values smaller than 20 % up to the upper troposphere. Results in figure 2 indicate that the statistical uncertainty affecting temperature measurements is only 0.5 K in the boundary layer, while it progressively decreases above the boundary layer to get down to 0.3 K at 10 km for all three selected atmospheric reference models. Correspondingly, the statistical uncertainty affecting relative humidity measurements ranges between 10 % in the boundary layer and 30 % in the upper troposphere. Simulations also reveal that the atmospheric boundary layer depth can be determined with a precision of 200 m, vertical profiles of particle backscatter & extinction with a precision of 5-20 %, while cloud geometrical properties and optical depth with a precision of 50-100 m and 5 %, respectively.

## References

- [1] Wulfmeyer, V., R. M. Hardesty, D. D. Turner, A. Behrendt, M. P. Cadeddu, P. Di Girolamo, P. Schlüssel, J. Van Baelen, and F. Zus, 2015: A review of the remote sensing of lower tropospheric thermodynamic profiles and its indispensable role for the understanding and the simulation of water and energy cycles, *Rev. Geophys.* **53**, 819–895.
- [2] Behrendt, A., Nakamura, T., Onishi, M., Baumgart, R., and Tsuda, T., 2002: Combined Raman lidar for the measurement of atmospheric temperature, water vapor, particle extinction coefficient, and particle backscatter coefficient, *Appl. Opt.* **41**, 7657–7666.
- [3] Behrendt, A., V. Wulfmeyer, E. Hammann, S.K. Muppa, and S. Pal., 2015: Profiles of second to third order moments of turbulent temperature fluctuations in the convective boundary layer: First measurements with rotational Raman lidar, *Atmos. Chem. Phys.* **15**, 5485-5500.
- [4] Di Girolamo, P., R. Marchese, D. N. Whiteman, and B. B. Demoz., 2004: Rotational Raman Lidar measurements of atmospheric temperature in the UV, *Geophys. Res. Lett.* **31**, L01106, ISSN: 0094-8276.
- [5] Di Girolamo, P., A. Behrendt, and V. Wulfmeyer, 2006: Spaceborne profiling of atmospheric temperature and particle extinction with pure rotational Raman Lidar and of relative humidity in combination with differential absorption Lidar: performance simulations, *Appl. Opt.* **45**, 2474-2494.
- [6] Di Girolamo, P., D. Summa, R. Ferretti, 2009: Multiparameter Raman Lidar Measurements for the Characterization of a Dry Stratospheric Intrusion Event, *J. Atmos. Ocean. Tech.* **26**, 1742-1762.
- [7] Radlach, M., A. Behrendt, and V. Wulfmeyer, 2008: Scanning rotational Raman lidar at 355 nm for the measurement of tropospheric temperature fields. *Atmos. Chem. Phys.* **8**, 159–169.
- [8] Hammann, E., A. Behrendt, F. Le Mounier, and V. Wulfmeyer, 2015: Temperature profiling of the atmospheric boundary layer with rotational raman lidar during the HD(CP)2 observational prototype experiment, *Atmos. Chem. Phys.* **15**, 2867-2881.
- [9] Whiteman, D. N., R. Kurt, R. Scott, 2010: Airborne and Ground-Based Measurements Using a High-Performance Raman Lidar, *J. Atmos. Ocean. Technol.* **27**(11), 1781–1801.
- [10] Wulfmeyer, V., H. Bauer, P. Di Girolamo, C. Serio, 2005: Comparison of active and passive water vapour remote sensing from space: An analysis based on the simulated performance of IASI and space borne differential absorption Lidar. *Remote Sens. Environ.* **95**, 211-230.
- [11] ESA, ARMA Reference Model of the Atmosphere, Tech. Rep. APP-FP/99-11239/AC/ac (European Space Agency, 1999).
- [12] Simonetti, F., A. Zuccaro Marchi, L. Gambicorti, V. Bratina, P. Mazzinghi, 2010: *Opt. Eng.* **49**, 073001.
- [13] Hammann E., and A. Behrendt, 2015: Parametrization of optimum filter passbands for rotational Raman temperature measurements, *Opt. Express* **23**, 30767-30782.